JAIDM
Journal of AI and Data Mining
Vol. 2, No .1, 2014, 39-52.

Solution of multi-objective optimal reactive power dispatch using pareto optimality particle swarm optimization method

S.A. Taher, M. Pakdel

Department of Electrical Engineering, University of Kashan, Kashan, Iran

Received 23 February 2013; accepted 13 July 2013
**Corresponding author: sataher@kashanu.ac.ir (S.A. Taher).).*

Abstract
For Multi-Objective Optimal Reactive Power Dispatch (MORPD), a new approach is proposed as a simultaneous minimization of the active power transmission loss, the bus voltage deviation and the voltage stability index of a power system are obtained. Optimal settings of continuous and discrete control variables (e.g., generator voltages, tap positions of tap changing transformers and the number of shunt reactive compensation devices to be switched) are determined. MORPD is solved using Particle Swarm Optimization (PSO). Also, Pareto Optimality PSO (POPSO) is proposed to improve the performance of the multi-objective optimization task defined with competing and non-commensurable objectives. The decision maker requires to manage a representative Pareto-optimal set provided by imposition of a hierarchical clustering algorithm. The proposed approach was tested using IEEE 30-bus and IEEE 118-bus test systems. When simulation results are compared with several commonly used algorithms, they indicate better performance and good potential for their efficient applications in solving MORPD problems.

Keywords: *Optimal reactive power dispatch, Particle swarm optimization, Multi-objective, Pareto optimality, Voltage profile, Voltage stability.*

1. Introduction

The Optimal Reactive Power Dispatch (ORPD) has played significant roles in the security and economics of power systems. Using this, the operators can select a number of control tools such as switching reactive power compensators, changing generator voltages and adjusting transformer tap settings, and achieving the Optimal Power Flow (OPF). Considering the given set of physical and operating constraints involved, the equality constraints include power flow equations and the inequality restrictions in various reactive power sources. ORPD objective is to minimize the transmission loss of the power system, keep the voltage profiles within acceptable range and improve the voltage security while satisfying certain operation constraints. However, as the transmission networks have tended to become stressed in a large number of utilities across the globe due to a variety of reasons, many voltage collapse accidents have occurred over the last few decades. Hence, voltage security has been considered in ORPD. The generator voltages are continuous variables, and the transformer ratios and shunt capacitors/inductors are discrete ones. The problem, therefore, has been defined as a non-linear, multi-uncertainty, multi-constraint, multi-minimum and multi-objective optimization (MOO) problem with a mixture of discrete and continuous variables.

A number of mathematical models for ORPD have been proposed in the literature [1–6]. Most of them adopt single-objective function and minimize it including transmission loss of the power system. Recently, minimizing voltage deviation from the desired values and improving voltage stability margin are considered as the objective function, making ORPD therefore, a MOO exercise [7–10]. In previous works, power losses and voltage deviation have received comparatively more attention than improving voltage stability. In this study, ORPD is similarly formulated as a MOO exercise with the objectives containing all three indices mentioned above as well as the operating constraints and load constraints.

Mathematical optimization techniques used to solve ORPD [1, 2, 7, 8] include gradient-based algorithms, linear programming, non-linear programming, Newton method and interior point methods. These conventional techniques require many mathematical assumptions, and hence, for problems involving non-continuous and non-linear functions, these techniques become less effective and are hardly ever used in recent years.

In recent decades, stochastic and heuristic optimization techniques, such as Evolutionary Algorithms (EAs), have emerged as efficient optimization tools [11]. EAs however, have been extensively employed for solving reactive power optimization [3–6, 9–10, 12-13]. Some of the prominent ones include Genetic Algorithm (GA) [14], particle swarm optimization (PSO) [15–19], differential evolution (DE) [20–22], seeker optimization algorithm (SOA) [23] and non-dominated sorting genetic algorithm-II (NSAGA-II) [24–25]. Theoretically, these techniques are able to converge to the near global optimum solution. PSO [26] was first suggested by Kennedy and Eberhart in 1995, and was subsequently employed successfully in power system studies for such applications as reactive power, voltage control, OPF, dynamic security border identification and state estimation [27–30].

Reviewing most studies to date, seems interesting to note that ORPD is not treated as a true multi-objective problem [18–19, 23], but instead, by linear combination of different objectives as a weighted sum, ORPD in effect has been often converted to a single objective problem. This unfortunately, requires multiple runs, as many times as the number of desired Pareto-optimal solutions. Furthermore, this method cannot be used to find Pareto-optimal solutions in problems having a non-convex Pareto-optimal front. In addition, there is no rational basis of determining adequate weights and the objective function formed might lose the significance due to combining non-commensurable objectives. To avoid this difficulty, in this study, the concept of Pareto-optimal set or Pareto-optimal front for MOO was presented as adopted in several works presented in the literature [9, 24–25]. This method is based on optimization of the most preferred objective while considering the other objectives as constraints bounded by some allowable levels. These levels are then altered to generate the entire Pareto-optimal set. The most obvious weaknesses of this approach are time-consuming and finding weakly non-dominated solutions [31]. There are reports of Pareto optimization method being used to solve the reactive power optimization problem [9, 32], or to design the power system stabilizer [33].

In this paper, an approach is proposed based on Pareto Optimality PSO (POPSO) whose effectiveness is verified in solving a multi-objective ORPD (MORPD) by simulating results of two standard test systems, including IEEE 30-bus and IEEE 118-bus power systems. When comparing the study results with previous works, POPSO was shown to perform well in both test systems by showing the solutions near global optima.

2. Problem formulation

2.1. Objective functions

The objective functions for both ORPD and voltage control problem comprise three important terms in which technical and economic goals are considered. The economic goal is mainly to minimize the active power transmission loss. The technical goals are to minimize the load bus voltage deviation from the desired voltage and also the *L*-index to improve the voltage security [18].

2.1.1. Power loss

Minimizing the active power transmission loss can be described as follows [18]:

$$\textbf{Min}\ \ P_{loss} = \sum_{k=1}^{N_E} Loss_k \tag{1}$$

Where, P_{loss} is the active power transmission loss of the power system, N_E is the number of branches and $Loss_k$ is the power losses of the k^{th} branch.

2.1.2. Voltage deviation

An effective way to improve voltage profile is to minimize the selected deviation of voltage from the desired value as follow [18]:

$$\textbf{Min}\ \ \sum \Delta V = \sum_{i=1}^{N_L} |V_i - V_i^{ref}| \tag{2}$$

Where, $\sum \Delta V$ is the sum of load bus voltage deviation, N_L is the total number of the system load buses, Vi and V_i^{ref} are actual and desired voltage magnitudes at bus i, respectively. In general, V_i^{ref} is set to be 1.0 pu.

2.1.3. Voltage stability index

There are several indices proposed for voltage stability and voltage collapse prediction, including:

voltage collapse proximity indicator (*VCPI*) [34] or voltage stability margin (*VSM*) [35]. However, *L*-index is a faster one presented by Kessel and Glavitsch [36] and developed further by Tuan et al [37]. In this paper, *L*-index is selected as the objective function for voltage stability index to improve the voltage security and keeps the operating system as far as possible from the voltage collapse point. Apart from the speedy calculation time needed to evaluate each load bus steady state voltage stability level, the chosen index can also take into account generator buses reaching reactive power limits. The *L*-index value ranges from zero to one; zero indicating a stable voltage condition (i.e. no system load) and one indicates voltage collapse. The bus with the highest *L*-index value will be the most vulnerable bus and hence, this method helps identifying the weakest areas needing critical reactive power support in the system. A summary of how *L*-index algorithm is evaluated is given below [18, 36]:
The transmission system itself is linear and allows a representation in terms of the node admittance matrix (*Y*). The network equations in this terms is:

$$\begin{bmatrix} I^L \\ I^G \end{bmatrix} = \begin{bmatrix} Y_1 & Y_2 \\ Y_3 & Y_4 \end{bmatrix} \cdot \begin{bmatrix} V^L \\ V^G \end{bmatrix} \quad (3)$$

Two categories of nodes are recognized: the load bus (PQ) set α_L and the generator bus (PV) set α_G. The hybrid matrix (*H*) can be generated from admittance matrix (*Y*) by a partial inversion as below:

$$\begin{bmatrix} V^L \\ I^G \end{bmatrix} = H \cdot \begin{bmatrix} I^L \\ V^G \end{bmatrix} = \begin{bmatrix} Z^{LL} & F^{LG} \\ K^{GL} & Y^{GG} \end{bmatrix} \cdot \begin{bmatrix} I^L \\ V^G \end{bmatrix}, \quad (4)$$

Where, V^L and I^L are vectors of voltages and currents at PQ buses; V^G and I^G are vectors of voltages and currents at PV buses; Z^{LL}, F^{LG}, K^{GL}, Y^{GG} are sub-matrices.
For any consumer node *j*, *j* v α_L, the following equation for V_j can be derived from the *H*-matrix:

$$V_j = \sum_{i \in \alpha_L} Z_{ji} . I_i + \sum_{i \in \alpha_G} F_{ji} . V_i \quad (5)$$

Voltage V_{oj} however, is been defined as:

$$V_{oj} = -\sum_{i \in \alpha_G} F_{ji} . V_i \quad (6)$$

Hence, the local indicator Lj becomes [36]:

$$L_j = \left| 1 - \frac{V_{oj}}{V_j} \right| = \left| 1 - \frac{\sum_{i \in \alpha_G} F_{ji} V_i}{V_j} \right| \quad (7)$$

Where, V_i and V_j are the complex voltages, and F_{ji} are the coefficients taken from a so-called *H* matrix, generated by a partial inversion of the nodal admittance matrix and the coefficients describe the system structure.
For stable situations the condition $0 \le L_j \le 1$ must not be violated for any of the nodes *j*. Hence, a global indicator *L* describing the stability of the whole system may be described as:

$$L = \max_{j \in \alpha_L}(L_j) \quad (8)$$

The *L* value for the best individual is compared with the threshold value and if the value is less than that, it indicates a voltage secure condition. The threshold value is fixed by conducting off-line study on the system for different operating conditions, thereby, minimizing the system voltage indicator [18] that is:

$$\text{Min } f_3 = L \quad (9)$$

2.2. Constraints

Minimizing the said objective functions is subjected to a number of equality and inequality constraints as outlined below.

2.2.1. Equality constraint

This is essentially the load constraint, i.e. the active and reactive power balance described by the following set of power flow equations [18, 19]:

$$\begin{cases} 0 = P_i - V_i \sum_{j \in N_L} V_j (G_{ij} \cos\theta_{ij} + B_{ij} \sin\theta_{ij}), & i = 1, \dots, N_{B-1} \\ 0 = Q_i - V_i \sum_{j \in N_L} V_j (G_{ij} \sin\theta_{ij} - B_{ij} \cos\theta_{ij}), & i = 1, \dots, N_{PQ} \end{cases}$$

(10)

Where, V_i is the voltage magnitude at i^{th} bus, P_i and Q_i are net active and reactive power injection at bus *i*, G_{ij} and B_{ij} are the mutual conductance and susceptance between bus *i* and *j* respectively, θ_{ij} is the voltage angle difference between bus *i* and *j*, N_{B-1} is the total number of buses excluding slack bus, N_{PQ} is the set of *PQ* buses and N_L is the number of load buses.

2.2.2. Inequality constraint

Sometimes referred to as the operational constraint, this includes the generator voltages V_G, shunt compensations Q_C, transformer tap settings *T*, generator reactive power outputs Q_G and load bus voltages V_L defined as [18, 19]:

$$\begin{cases} V_{Gi\min} \le V_{Gi} \le V_{Gi\max}, & i = 1, \dots, N_G \\ Q_{Ci\min} \le Q_{Ci} \le Q_{Ci\max}, & i = 1, \dots, N_C \\ T_{i\min} \le T_i \le T_{i\max}, & i = 1, \dots, N_T \\ Q_{Gi\min} \le Q_{Gi} \le Q_{Gi\max}, & i = 1, \dots, N_G \\ V_{Li\min} \le V_{Li} \le V_{Li\max}, & i = 1, \dots, N_L \end{cases} \quad (11)$$

Where, N_G, N_C, N_T and N_L are the total number of generators, shunt compensations, transformer taps and load buses, respectively.

2.3. Problem statement

In general, considering aggregation of objectives and constraints, power loss, voltage control and voltage stability index could be mathematically formulated as a non-linear constrained MOO as described below [18]:

$$\left.\begin{array}{ll} Min & P_{loss}(x,u) \\ Min & \sum \Delta V\,(x,u) \\ Min & L(x,u) \\ s.t. & \\ & H(x,u)=0 \\ & G_{\min}(x,u)\le G(x,u)\le G_{\max}(x,u) \end{array}\right\} \quad (12)$$

Where, x is the state variable vector, consisting of load bus voltages V_L and generator reactive power outputs Q_G; u is the control variable vector including generator voltages V_G, shunt compensations Q_C and transformer tap settings T. $H(x,u)$ and $G(x,u)$ are the compact forms of Eqs. (10) and (11), respectively.

3. Pareto Optimality Particle Swarm Optimization (POPSO)

3.1. Classical particle swarm optimization

PSO is a stochastic evolutionary computation optimization technique based on the movement of swarms [26]. It was inspired by social behavior of bird flocking or fish schooling. The population is considered as swarm, and each individual is called a particle randomly initialized. Each of these particles traverses the search space looking for the global minimum or maximum. The position of each particle corresponds to a candidate solution for the optimization problem, and is treated as a point in a D-dimensional space. For a given particle P_i, its position and velocity are represented as $x_i(t)=(x_{i,1}(t),\ldots,x_{i,d}(t),\ldots,x_{i,D}(t))$ and $v_i(t)=(v_{i,1}(t),\ldots,v_{i,d}(t)\ ,\ldots,v_{i,D}(t))$, respectively. The particles have memory and each particle keeps track of its previous best position. The best previous position (the position giving the best fitness value) found so far by particle P_i is recorded as $pbest_i=(p_{i,1},\ldots,p_{i,d},\ldots,p_{i,D})$. The swarm remembers another value which is the best position discovered by the swarm, The best previous position among all the particles in the population (or in the neighborhood) is represented as $gbest=(g_{i,1},\ldots,g_{i,d},\ldots,g_{i,D})$. The velocity for particle and the their positions are updated by the following two equations [18, 26]:

$$v_{i,d}(t+1)=w\times v_{i,d}(t)+c_1\times rand_1\times(pbest_{i,d}(t)-x_{i,d}(t))+ c_2\times rand_2\times(gbest_d(t)-x_{i,d}(t)) \quad (13)$$

$$x_{i,d}(t+1)=x_{i,d}(t)+v_{i,d}(t+1) \quad (14)$$

Where, w is the inertia weight, c_1 and c_2 are learning factors, $rand_1$ and $rand_2$ are two random functions in the range [0, 1]. The Eq. (13) is used to calculate the i^{th} particle's velocity by taking three terms into consideration: the particle's previous velocity, the distance between the particle's best previous and current positions, and, finally, the distance between the position of the best particle in the swarm and the i^{th} particle's current position. The i^{th} particle flies toward a new searching point according to Eq. (14). In general, the performance of each particle is measured by a predefined problem-dependent fitness function.

PSO has three tuning parameters and the performance of its algorithm is influence by them. The parameters are w, c_1 and c_2 shown in Eq. (13). w is the inertia weight employed to control the impact of the previous history of velocities on the current one. Suitable selection of the inertia weight w can provide a balance between global and local exploration abilities, consequently on average less iteration is needed to find a sufficiently optimal solution [38]. The linearly decreasing w-strategy [39] decreases from w_{max} to w_{min}, according to the following equation:

$$w=w_{\max}-\frac{w_{\max}-w_{\min}}{iter_{\max}}\times iter \quad (15)$$

Where, $iter$ is the current iteration number and $iter_{max}$ is the maximum iteration number, w_{max} and w_{min} often set to 0.9 and 0.4, also c_1 and c_2 are the learning factors and determine the influence of personal best $pbest_i$ and global best $gbest$, respectively shown in Eq. (13). Most implementations [26–30] use a setting with $c_1 = c_2 = 2$, which means each particle will be attracted to the average of $pbest_i$ and $gbest$. Recently, reports show that it might be even better to choose a larger cognitive parameter c_1 than a social parameter c_2, but with this constraint $c_1+c_2\le 4$ [40].

The number of particles or swarm size N_{pop} is one of the most important parameters that influence results of PSO. Too few particles will cause the algorithm to become stuck in a local minimum, while too many particles will slow down the algorithm. The algorithm performance depends therefore, on the parameters and the functions being optimized, so it is important to find a set of parameters that work well in all cases [18].

3.2. Pareto optimality concept

Optimization of several objective functions simultaneously, takes place frequently in power system studies. Generally, these functions are non-commensurable and often have conflicting objectives. There are two approaches for solving MOO problems. First, is the application of the traditional algorithms aiming to convert the multi-objective to a single objective optimization problem, often carried out by aggregating all objectives in a weighted function, or simply transforming all but one of the objectives into constraints. The advantage of such an approach is application existing single-objective optimization algorithms to solve problem directly and the limitations include: 1) requiring a pre-knowledge on the relative importance of the objectives and their limitations which are being converted into constraints; 2) inability to find multiple solutions in a single run, thereby requiring it to be applied as often as the number of desired Pareto optimal solutions; 3) difficulty in evaluating the trade-off between objectives and 4) search space should be convex, otherwise the solution may not be attainable. The second approach is based on Pareto optimality (PO) concept, where a set of optimal solutions is found, instead of one optimal solution. The reason for the optimality of many solutions is that no one can be considered to be better than any other with respect to all objective functions. Compared with traditional algorithms, PO is more suitable for solving MOO not only due to the ability to obtain multiple solutions in a single run, but, a good spread of the non-dominated solutions can also be obtained [41].

The following definitions describe concept of Pareto-optimal mathematically [41]:

Def. 1 The general MOO problem consists of a number of objectives to be optimized simultaneously and is associated with a number of equality and inequality constraints. It can be formulated as follows:

$$\left.\begin{array}{ll} Min & \vec{y}=\vec{F}(\vec{x})=[\vec{f}_1(\vec{x}),\vec{f}_2(\vec{x}),\dots,\vec{f}_{N_{obj}}(\vec{x})]^T \\ s.t. & \vec{H}_j(\vec{x})=0 \\ & \vec{G}_j(\vec{x})\le 0,\ j=1,2,\dots,M \end{array}\right\} \quad (16)$$

Where, $\vec{x}^*=[\vec{x}_1^*,\vec{x}_2^*,\dots,\vec{x}_D^*]\in\Omega$ and $\vec{y}$ is the objective vector. Here, three functions are considered including: $\vec{f}_1(\vec{x})=P_{Loss}(x,u)$, $\vec{f}_2(\vec{x})=\sum\Delta V\,(x,u)$ and $\vec{f}_3(\vec{x})=L\,(x,u)$.

$\vec{H}_j(\vec{x})$ is equality constraint including active and reactive power balance. $\vec{G}_j(\vec{x})$ are un-equality constraints, includes the generator voltages, shunt compensations, transformer tap settings, generator reactive power outputs and load bus voltages. $\vec{x}^*$ is a D-dimensional vector representing the decision variables within a parameter space Ω and N_{obj} is the number of objectives. The space spanned by the objective vectors is called the objective space. The subspace of the objective vectors satisfying the constraints is called the feasible space.

Def. 2 For a MOO problem, any two solutions can have one of two possibilities, one covers or dominates the other or none dominates the other. In a minimization problem, without loss of generality, a decision vector $\vec{x}_1\in\Omega$ is said to dominate the decision vector $\vec{x}_2\in\Omega$ (denoted by $\vec{x}_1\prec\vec{x}_2$), if the decision vector $\vec{x}_1$ is not worse than $\vec{x}_2$ in all objectives and strictly better than $\vec{x}_2$ in at least one objective. Therefore, a solution $\vec{x}_1$ dominates $\vec{x}_2$ if the following conditions are satisfied:

$$\begin{cases}\forall i\in\{1,2,\dots,N_{obj}\}: \vec{f}_i(\vec{x}_1)\le\vec{f}_i(\vec{x}_2) \\ \exists j\in\{1,2,\dots,N_{obj}\}: \vec{f}_j(\vec{x}_1)<\vec{f}_j(\vec{x}_2)\end{cases} \quad (17)$$

Def. 3 A decision vector $\vec{x}_1\in\Omega$ is called Pareto-optimal, if there does not exist another $\vec{x}_2\in\Omega$ that dominates it. An objective vector is called Pareto-optimal, if the corresponding decision vector is Pareto-optimal.

Def. 4 The set of all non-dominated solutions is called Pareto optimal set (POS) and the set of the corresponding values of the objective functions is called Pareto optimal front (POF) or simply Pareto front. In case of no non-dominated solution, Pareto optimal front would be non-convex.

PO is shown graphically in Figure 1 for an arbitrary two-objective minimization problem. It is apparent that for solutions contained in dominated regions, there exists at least one solution in the non-dominated region that is strictly better in terms of both objectives. Furthermore, each non-dominated solution is obviously not inferior to any solution within the entire search space.

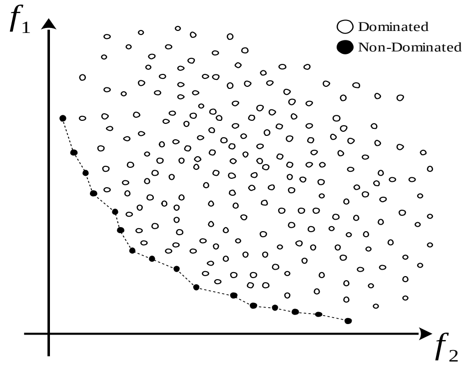

Figure 1. Depiction of domination using a two-objective minimization case

3.2.1. Best compromise solution (BCS)

From the Pareto-optimal set of non-dominated solutions, the proposed POPSO selects one solution for the decision maker as the best compromise solution. For this optimization, due to the imprecise nature of the decision making process involved, the i^{th} objective function F_i is represented by a membership function μ_i defined as [9, 42]:

$$\mu_i = \begin{cases} 1 & F_i \le F_{i,\min} \\ \dfrac{F_{i,\max} - F_i}{F_{i,\max} - F_{i,\min}} & F_{i,\min} < F_i < F_{i,\max} \\ 0 & F_i \ge F_{i,\max} \end{cases} \quad (18)$$

Where, $F_{i,\min}$ and $F_{i,\max}$ are the minimum and maximum value of the i^{th} objective function among all non-dominated solutions, respectively. For each non-dominated solution k, the normalized membership function μ^k is calculated as:

$$\mu^k = \frac{\sum_{i=1}^{N_{obj}} \mu_i^k}{\sum_{k=1}^{M} \sum_{i=1}^{N_{obj}} \mu_i^k} \quad (19)$$

Where, M is the number of non-dominated solutions. Here, the best compromise solution is the one with the maximum μ^k.

4. Solution algorithm

The difficulty in extending the original PSO to POPSO is the selection of *pbest* and *gbest* for each particle, since no single optimum solution in Pareto optimal set exist. The algorithm uses an archive, which is in essence an external repository of the population, storing non-dominated solutions. Initializing randomly the population starts the algorithm. All particles are initially compared with each other in order to store the non-dominated ones in the archive. Particles velocity and positions are updated using Eqs. (13-14) for which $gbest_d$ is randomly selected from the global Pareto archive for each particle, therefore $gbest_d$ is transformed to $gbest_{i,d}$. It means that *gbest* is exclusive for each particle. As for the $pbest_{i,d}$, the first value is set equal to the initial position of particle. In the subsequent iterations, $pbest_{i,d}$ is updated in the following stages:

(I) if the current $pbest_{i,d}(t)$ dominates the new position $x_{i,d}(t+1)$ then $pbest_{i,d}(t+1)= pbest_{i,d}(t)$,

(II) if the new position $x_{i,d}(t+1)$ dominates $pbest_{i,d}(t)$ then $pbest_{i,d}(t+1)= x_{i,d}(t+1)$,

(III) if no one dominates the other, then, one of them is randomly selected to be the $pbest_{i,d}(t+1)$.

Contrary to standard PSO, where a best solution is obtained, there are several equally good non-dominated solutions stored in the POPSO archive. In every iteration t, the new positions of all particles are compared to identify the non-dominated ones, which are then compared further with all solutions stored in the archive. Following updating the archive, new non-dominated solutions are added and old solutions that have become dominated are eliminated. The size of the archive is therefore, an important parameter, which needs to be determined accordingly. Once the archive becomes full, a new non-dominated solution is found. Then this new solution replaces another non-dominated solution randomly selected in the archive. In this article, no limit has been considered for the archive size. The algorithm runs until the maximum number of iterations is reached. Below, the proposed POPSO algorithm for solving the MORPD is discretely described in steps:

Step 1: Input data

Input power system data and parameter values such as inertia weight w and learning factors c_1 and c_2 in the appropriate equations.

Step 2: Initialization

(I) Initialize randomly the position and initial velocity of the particles. Each particle in the population consists of D component, where D is the number of space dimensions indicating the number of control variables such as generator voltages, transformer taps and shunt reactive compensations. Select and verify each particle for constraints; if the particle doesn't satisfy the relevant constraints, then regenerate another one.

(II) Compute the multi-objective functions (P_{loss}, $\sum \Delta V$ and L-index) for each particle and its relevant constrains using power flow algorithm such as Newton Raphson method; then save this in a vector form.

(III) Check the PO of each particle, and store non-dominated particles in Pareto archive. If the specific constraint doesn't exist for archive, the size of the archive is assumed unlimited.

Step 3: Updating

(I) Update velocity and positions of particles according to Eqs. (13-14); $gbest_{i,d}(t)$ is randomly selected from the Pareto archive for each particle.

(II) Update $pbest_{i,d}(t+1)$ for each particle according to checking the PO of $pbest_{i,d}(t)$ and $x_{i,d}(t+1)$. If no one dominates the other, then, one of them is randomly selected to be the $pbest_{i,d}(t+1)$.

(III) If the particle doesn't remain within the feasible solution region, discard it and mutate again.

Step 4: Evaluation

Evaluate the multi-objective functions for each particle by power flow; and save it in a vector form.

Step 5: Selection and update the archive

(I) Check the PO of each particle. If the fitness value of the particle is non-dominated (compared to the Pareto optimal front in the archive), save it into the archive.

(II) If a particle is dominated from the new one in the Pareto archive, then discard it.

Step 6: Repeat

Repeat step 3 to step 5 until the maximum number of iterations is reached. The flowchart for the MORPD solution using POPSO is illustrated in Figure 2.

5. Simulation results

The proposed approach was tested with two non-linear test systems (IEEE 30-Bus and IEEE 118-Bus power system) for validation [43]. Basic information for test systems as well as control variable settings and limits are elaborated in Tables 1 and 2. The algorithm implemented in MATLAB and executed on a PC with a Pentium IV 2.1G CPU.

The following parameters are adopted in POPSO: population size = 100; inertia weight w which linearly decreases from 1 to 0.5; initial learning factors c_1 = 2.0 and c_2 = 1.6; desired number of generations = 50.

Table 1. Control variables of IEEE 30-bus and IEEE 118-bus test systems

Test system	Number of bus	Number of branch	Number of control variables		
			V_G	T	Q_C
IEEE 30-bus	30	41	6	4	4
IEEE 118-bus	118	186	54	14	9

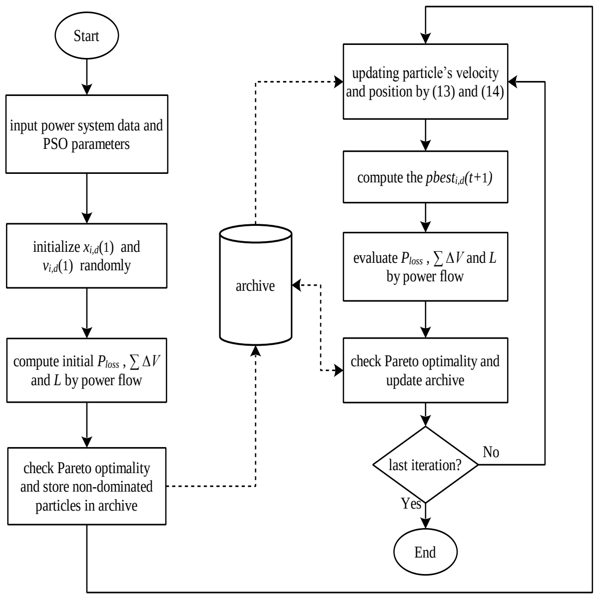

Figure 2. Flowchart for solving MORPD problem using POPSO.

Table 2. Control variable settings IEEE 30-bus and IEEE 118-bus test systems

Control variable	Control variable limits		Step
	Min (p.u.)	Max (p.u.)	
V_G	0.9	1.1	-
T	0.9	1.1	0.01
Q_C	0	0.5	0.01

5.1. Simulation of the IEEE 30-bus test system

The proposed POPSO method was tested on the standard IEEE 30-bus system shown in Figure 3. It consists of six generator buses (bus 1 being the slack bus, while buses number 2, 5, 8, 11 and 13 are PV buses with continuous operating values), 24 load buses and 41 branches in which four branches (4–12, 6–9, 6–10 and 27–28) are tap changing transformers with discrete operating values. In addition, buses 10, 15, 19 and 24 are taken as shunt compensation buses with discrete operating values. Therefore, in total, 14 control variables are taken for MORPD in this test system. Table 3 illustrates the simulation results for the IEEE 30-bus test system, where Pareto optimal front and Pareto optimal set are listed for 36 rows of non-dominated solutions. Table 4 shows the best compromise solution (BCS) and 3 solutions in Pareto optimal front that have minimum value for each objective function individually and are similar to single objective functions (Min P_{loss}, Min $\sum \Delta V$ and Min *L-index*). The diversity of the Pareto optimal front over the trade-off surface is also shown in Figure 4.

The variation of best compromise solution power loss, voltage deviation and voltage stability index versus the number of iterations are presented in Figures. 5-7, respectively. As can be seen, the convergence characteristics are not monotonic most likely due to the existence of best compromise solution (BCS). In the each iteration, there are several non-dominated solutions and one of them has been selected as BCS considering Eqs. (18-19). In the following iteration, however, one other solutions might be selected as BCS, therefore a non-monotonic convergence may occur. Pre and post optimization for bus voltage profiles are shown in Figure 8. As can be seen after optimization, the voltage profiles are greatly improved, and voltage deviations are reduced.

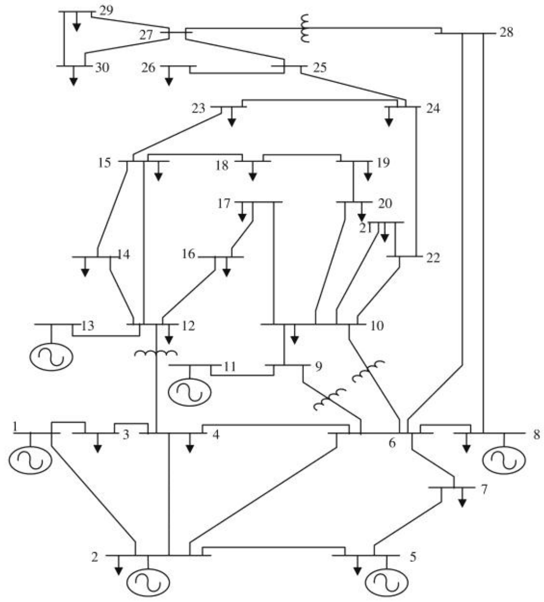

Figure 3. IEEE 30-bus test system

Table 3.The results of IEEE 30-bus test system

Pareto optimal front			Pareto optimal set													
P_{loss}	$\sum \Delta V$	L	V_{G1}	V_{G2}	V_{G5}	V_{G8}	V_{G11}	V_{G13}	T_{4-12}	T_{6-9}	T_{6-10}	T_{27-28}	Q_{C10}	Q_{C15}	Q_{C19}	Q_{C24}
5.1542	0.1080	0.1281	1.0446	1.0262	1.0190	1.0000	1.0293	0.9983	1.00	0.98	1.02	0.97	0.13	0.08	0.09	0.16
5.3292	0.0888	0.1296	1.0325	1.0400	1.0117	0.9855	1.0302	1.0024	0.99	0.98	1.04	0.95	0.10	0.09	0.09	0.20
4.5374	0.4512	0.1237	1.0974	1.0682	1.0784	1.0890	1.0154	1.0198	1.02	1.02	1.01	1.02	0.16	0.07	0.00	0.10
4.6244	0.3048	0.1207	1.0783	1.0683	1.0511	1.0502	1.0307	1.0252	1.04	1.00	1.03	1.00	0.15	0.07	0.04	0.07
4.6654	0.4320	0.1185	1.0819	1.0617	1.0757	1.0481	1.0433	1.0179	1.03	0.99	1.03	0.99	0.16	0.15	0.07	0.06
4.5190	**0.7968**	**0.1161**	**1.1000**	**1.0772**	**1.0712**	**1.0761**	**1.0499**	**1.0322**	**1.01**	**1.01**	**1.05**	**0.98**	**0.23**	**0.12**	**0.12**	**0.04**
4.9474	0.1776	0.1225	1.0542	1.0459	1.0365	1.0214	1.0283	1.0002	1.04	0.98	1.01	0.97	0.14	0.12	0.07	0.09
4.7983	0.2472	0.1216	1.0671	1.0414	1.0702	1.0545	1.0297	1.0012	1.01	1.00	1.00	0.98	0.17	0.05	0.06	0.08
5.2205	**0.0768**	**0.1339**	**1.0227**	**1.0339**	**1.0130**	**0.9977**	**1.0007**	**1.0021**	**1.02**	**1.00**	**1.00**	**0.95**	**0.21**	**0.13**	**0.07**	**0.13**
4.9473	0.1608	0.1237	1.0557	1.0304	1.0342	1.0166	1.0177	0.9889	1.00	0.99	1.02	0.97	0.12	0.10	0.09	0.15
5.1051	0.1056	0.1348	1.0430	1.0260	1.0410	1.0016	1.0257	0.9806	1.00	1.01	1.02	0.96	0.16	0.08	0.10	0.16
4.9142	0.1608	0.1247	1.0501	1.0382	1.0537	1.0197	1.0156	0.9846	1.00	1.01	1.01	0.97	0.15	0.12	0.05	0.16
4.8736	0.2472	0.1201	1.0756	1.0603	1.0543	1.0490	1.0347	1.0009	1.02	0.97	1.05	0.97	0.10	0.01	0.09	0.07
4.8666	0.1824	0.1247	1.0579	1.0360	1.0648	1.0368	1.0134	1.0027	1.02	1.00	1.02	0.99	0.16	0.14	0.01	0.12
4.8522	0.1968	0.1234	1.0541	1.0520	1.0382	1.0306	1.0217	1.0035	1.02	1.00	1.03	0.99	0.18	0.10	0.07	0.09
4.6820	0.3000	0.1210	1.0800	1.0462	1.0741	1.0494	1.0292	1.0114	1.03	1.00	1.05	1.00	0.21	0.04	0.05	0.10
4.5216	0.6048	0.1173	1.0966	1.0754	1.0952	1.0819	1.0381	1.0272	1.03	0.99	1.04	1.01	0.17	0.05	0.06	0.10
4.9216	0.1848	0.1222	1.0594	1.0522	1.0532	1.0259	1.0239	0.9950	1.03	0.98	1.03	0.98	0.12	0.11	0.08	0.10
4.6692	0.3696	0.1185	1.0779	1.0723	1.0409	1.0485	1.0474	1.0150	1.02	0.99	1.03	0.99	0.18	0.05	0.05	0.09
4.6820	0.3336	0.1207	1.0884	1.0632	1.0736	1.0517	1.0321	1.0067	1.03	1.01	1.04	1.02	0.21	0.11	0.03	0.07
4.6423	0.3888	0.1201	1.0813	1.0763	1.0448	1.0631	1.0367	1.0124	1.02	1.01	1.04	1.01	0.20	0.14	0.03	0.04
4.6362	0.3576	0.1207	1.0771	1.0536	1.0480	1.0579	1.0325	1.0391	1.00	1.00	1.03	1.00	0.13	0.07	0.03	0.08
4.7256	0.3168	0.1191	1.0854	1.0475	1.0742	1.0576	1.0505	1.0114	1.00	0.98	1.04	1.00	0.14	0.08	0.00	0.06
4.6664	0.2808	0.1225	1.0783	1.0726	1.0711	1.0498	1.0291	1.0147	1.01	1.02	1.06	1.00	0.19	0.07	0.01	0.07
4.6828	0.4200	0.1179	1.0830	1.0807	1.0668	1.0500	1.0422	1.0195	1.02	0.99	1.05	1.01	0.20	0.13	0.02	0.06
4.6703	**0.2458**	**0.1192**	**1.0713**	**1.0372**	**1.0386**	**1.0433**	**1.0318**	**1.0301**	**1.04**	**0.99**	**1.01**	**1.00**	**0.10**	**0.04**	**0.05**	**0.08**
4.6917	0.4416	0.1164	1.0808	1.0756	1.0913	1.0694	1.0557	1.0223	1.02	0.97	1.04	0.97	0.11	0.06	0.07	0.03
4.6995	0.2400	0.1250	1.0712	1.0609	1.0445	1.0482	1.0140	1.0121	1.02	1.01	1.03	0.99	0.18	0.09	0.04	0.07
4.6090	**0.5208**	**0.1151**	**1.0864**	**1.0542**	**1.0698**	**1.0695**	**1.0587**	**1.0016**	**1.02**	**0.98**	**1.04**	**1.02**	**0.14**	**0.09**	**0.07**	**0.11**
4.7586	0.2520	0.1207	1.0784	1.0632	1.0459	1.0513	1.0327	0.9987	1.04	0.99	1.02	0.99	0.14	0.10	0.07	0.09
4.6423	0.3888	0.1201	1.0813	1.0763	1.0448	1.0631	1.0367	1.0124	1.01	1.01	1.04	1.01	0.20	0.14	0.03	0.04
4.7006	0.3288	0.1179	1.0868	1.0700	1.0652	1.0430	1.0452	1.0200	1.04	0.98	1.05	1.00	0.16	0.07	0.03	0.09
4.6882	0.2880	0.1222	1.0902	1.0726	1.0711	1.0498	1.0291	1.0147	1.01	1.01	1.06	1.00	0.19	0.07	0.01	0.06
4.7531	0.3048	0.1194	1.0800	1.0740	1.0692	1.0404	1.0363	1.0095	1.03	0.99	1.05	0.99	0.21	0.05	0.01	0.12
4.7257	0.2184	0.1247	1.0677	1.0568	1.0629	1.0329	1.0157	1.0226	1.02	1.02	1.04	1.00	0.20	0.05	0.04	0.11
4.6669	0.3648	0.1191	1.0800	1.0722	1.0750	1.0743	1.0272	1.0163	1.03	0.99	1.03	1.01	0.17	0.10	0.03	0.08

Table 4. Best compromise solution (BCS) and minimum value for each objective function

	P_{loss} (MW)	$\sum \Delta V$	L
BCS	*4.6703*	*0.2458*	*0.1192*
Min P_{loss}	**4.5190**	0.7968	0.1161
Min $\sum \Delta V$	5.2205	**0.0768**	0.1339
Min L	4.6090	0.5208	**0.1151**

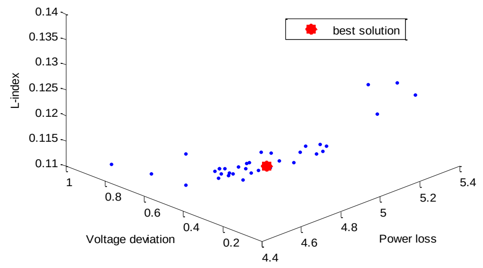

Figure 4. Pareto optimal front of the proposed approach

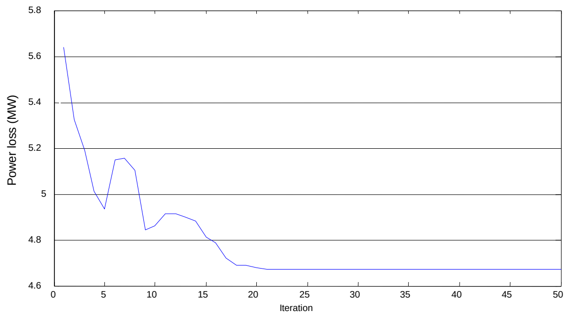

Figure 5. Convergence of best compromise solution power loss

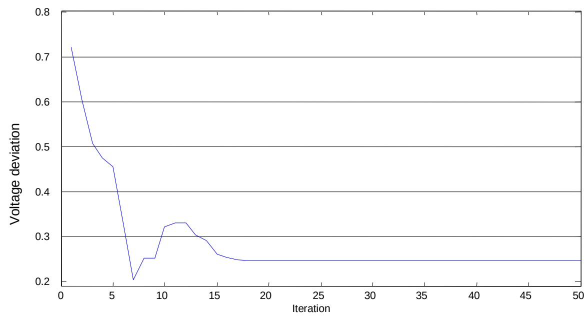

Figure 6. Convergence of best compromise solution voltage deviation

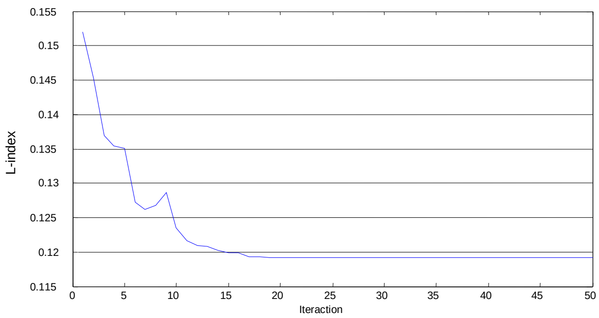

Figure 7. Convergence of best compromise solution voltage stability index

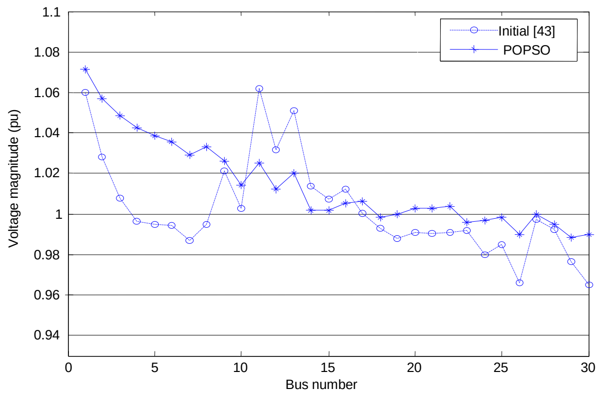

Figure 8. Bus voltage profiles

To evaluate the performance of proposed POPSO approach, the simulation results are compared with other listed algorithms in Table 5 as discussed below:

Comparing POPSO with initial case

The following points are noted: a) Active power losses before and after proposed POPSO optimization are 5.7213 (column 2 Table 5) and 4.6703 (column 11 Table 5), respectively, indicating a power loss reduction of 18.37%. b) Voltage deviation is also reduced from 0.7656 in the initial case to 0.2458, i.e. a reduction of 67.89%. c) Voltage stability index, too is reduced from 0.1563 to 0.1192 (i.e. 23.74%, improvement).

Comparing POPSO with PSO and FAPSO

The numerical results from Table 5 indicate that in the same test system, the BCS determined by POPSO is better than both PSO and FAPSO [18]. Here, the least improvement (reduction) achieved in power loss, voltage deviation and voltage stability index are 5.65%, 6.89% and 3.72%, respectively.

Comparing POPSO with CLPSO

In CLPSO technique, three cases with different objectives are considered [19]: Case 1, a single objective is defined to minimize the real power loss; Case 2, two objectives are defined in order to minimize the power loss and voltage deviation; and Case 3, where two objectives of minimizing the power loss and voltage stability index are defined. The best candidate in Pareto optimal front for comparing POPSO with CLPSO-Case 1 is Min P_{loss} in Table 4, where the solution for P_{loss} is 4.519 which compared to the latter (i.e. 4.5615) indicates slight improvement in working with POPSO. BCS is chosen in this study for comparing POPSO and CLPSO-Case 2 and CLPSO-Case 3. Only voltage deviation in CLPSO-Case 2 is slightly less than POPSO, but POPSO still illustrates better results with respect to other specification. Comparing CLPSO-Case 3 with POPSO, P_{loss} and voltage deviation are still inferior for the former. It is worth mentioning that in [19], the number of shunt compensations employed in CLPSO's is 9, while in this paper we have used 4. This may cause L index to be less than the case considered for POPSO comparisons (in CLPSO-Case 3, L index is 0.0866 against 0.1192 for POPSO).

Comparing POPSO with DE

In DE algorithm [22], three cases (Case 1: minimization of system power loss, Case 2: improvement of voltage profile and Case 3: enhancement of voltage stability) with different objectives are considered as follows: for minimizing real power loss, the best candidate at Pareto optimal front for comparison is for Min P_{Loss} in POPSO is 4.519 (column 2, Table 4) against 4.555 for DE (0.036 MW loss reduction) and as can be seen POPSO shows improvement over DE in all other specs, too (at least 78.38% improvement in $\sum \Delta V$ and L). Also, the best candidate at Pareto optimal front for comparison with DE-Case 2 and DE-Case 3 (Min $\sum \Delta V$ and Min L) are 0.0768 (column 3, Table 4) against 0.0911 for voltage deviation, and 0.1151 (column 4, Table 4) against 0.1246 for voltage stability, respectively (at least 15.69% and 7.62% improvement are observed in voltage profile and voltage stability index, respectively).

Comparing POPSO with NSGA-II and MNSGA-II

NSGA-II and MNSGA-II are algorithms that use Pareto optimality for MOO. Minimizing the power loss and voltage stability index could be defined as the two objectives of ORPD [25]. Best P_{Loss} and best L are Pareto optimal front solutions, each representing a minimum objective function for power loss and voltage stability index. The best candidates at Pareto optimal front for comparing POPSO with NSGA-II and MNSGA-II are Min P_{loss} for Best P_{Loss} and Min L for Best L. Advantage of POPSO with respect to NSGA-II and MNSGA-II are expressed in Table 5, where BCS indicate improvement in power loss and voltage stability index of at least 5.69% and 13.75%, respectively.

Figures 9-11, clearly compares the results of proposed POPSO with other methods for IEEE 30-bus test system. Therefore, as can be seen, the proposed POPSO method yields nearer global optimal solution for both single and multi-objectives.

5.2. Simulation of the IEEE 118-bus test system

In order to evaluate the applicability of the proposed method to bigger systems, IEEE 118-bus power system is employed which consists of 54 generator buses, 64 load buses and 186 branches in which 14 branches are tap changing transformers with discrete operating values. In addition, 9 buses are taken as shunt compensation buses with discrete operating values. In this system, a total of 77 control variables are taken for MORPD.

Table 6 and Figures 12-15 show the results obtained by the proposed POPSO when compared with other methods [18, 19, 25, 43] where improvement in power loss, voltage deviation and voltage stability index are at least 1.26%, 3.3% and 8.27%, respectively, and can therefore be efficiently used for the MORPD problem. Again, it is worth noting that in [19], the number of shunt compensations employed in CLPSO's is 14, and in this paper we have used 9. The same argument for L index as outlined above applies here too (in CLPSO-Case 3, L index is 0.0965 against 0.1087 for POPSO).

6. Conclusion

In this paper, a new approach based on POPSO has been proposed and applied to MORPD problem. The problem has been formulated as MOO problem with competing power loss, bus voltage deviation and voltage stability index. A hierarchical clustering technique is implemented to provide the operator with a representative and manageable Pareto optimal set without destroying the characteristics of the trade-off front. Moreover, a proposed mechanism is employed to extract the best compromise solution over the trade-off curve. The Pareto multi-objective algorithms here implemented have the advantage of including multiple criteria without the need for introducing weights in a simple aggregating function. The results show that the proposed approach is efficient for solving MORPD problem where multiple Pareto optimal solutions can be found in one simulation run. The algorithms have been tested for standard IEEE 30-bus and 118-bus test systems and results are compared with others commonly used algorithms in the literature. Comparison shows that the proposed approach performed better than the other algorithms and can be efficiently used for the MORPD problem as near global optimum solutions reached in this study. The comparison seems to dominate other algorithms results.

Table 5. Comparison of POPSO with other techniques on IEEE 30-bus test system

	Initial [43]	PSO [18]	FAPSO [18]	CLPSO [19]			DE [22]			NSGA-II [25]		MNSGA-II [25]		POPSO
				Case 1	Case 2	Case 3	Case 1	Case 2	Case 3	Best P_{loss}	Best L	Best P_{loss}	Best L	(BCS)
P_{loss}(MW)	5.7213	5.1600[a]	4.9500[a]	4.5615	4.6969	4.6760	4.555	6.4755	7.0733	4.952	5.128	4.9454	5.102	**4.6703**
$\sum\Delta V$	0.7656	0.3840[b]	0.2640[b]	0.4773	0.2450	0.5171	1.9589	0.0911	1.4191	-	-	-	-	**0.2458**
L	0.1563	0.1307	0.1238	0.1230	0.1247	0.0866	0.5513	0.5734	0.1246	0.1393	0.1382	0.13940	0.1382	**0.1192**

[a] P_{loss}(p.u.)$\times$ 100=P_{loss} (MW)
[b] ΔV(p.u.) $\times N_L$=$\sum\Delta V$

Table 6.The results of POPSO and comparison with other methods on IEEE 118-bus test system

	Initial [43]	PSO [18]	FAPSO [18]	CLPSO [19]			NSGA-II [25]		MNSGA-II [25]		POPSO
				Case 1	Case 2	Case 3	Best P_{loss}	Best L	Best P_{loss}	Best L	(BCS)
P_{loss}(MW)	133.14	117.81	115.37	130.96	132.06	132.08	119.57	132.21	119.279	132.17	**113.92**
$\sum\Delta V$	2.0150	0.7488	0.7744	1.8525	1.6177	2.8863	-	-	-	-	**0.7241**
L	0.1497	0.1295	0.1185	0.1461	0.1210	0.0965	0.4553	0.4113	0.4553	0.4074	**0.1087**

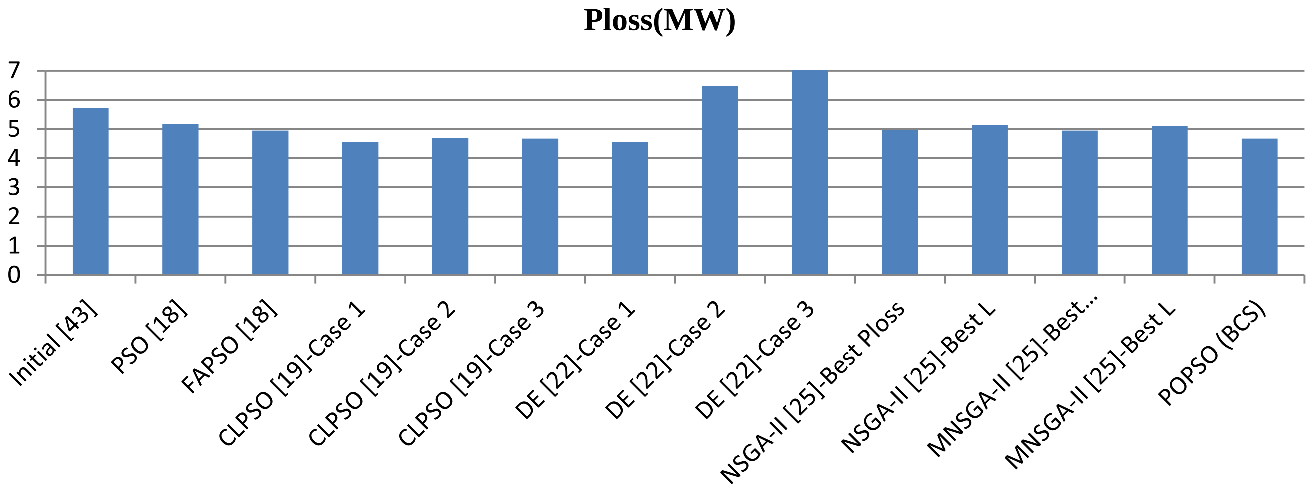

Figure 9. Comparison results of power loss in IEEE 30-bus test system

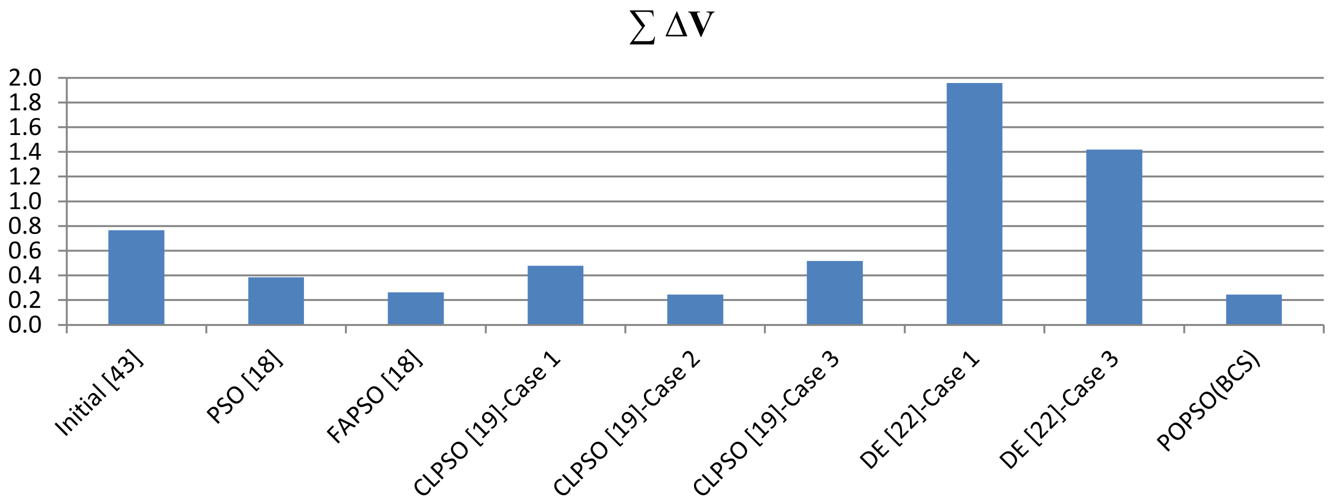

Figure 10. Comparison results of voltage deviation in IEEE 30-bus test system

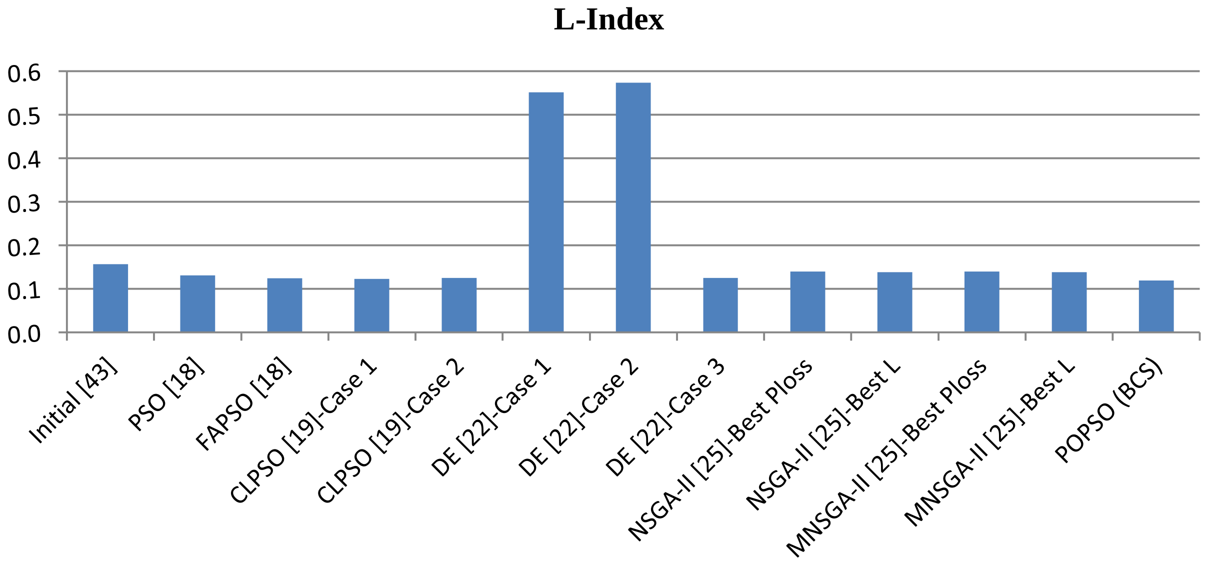

Figure 11. Comparison results of *L*-index in IEEE 30-bus test system

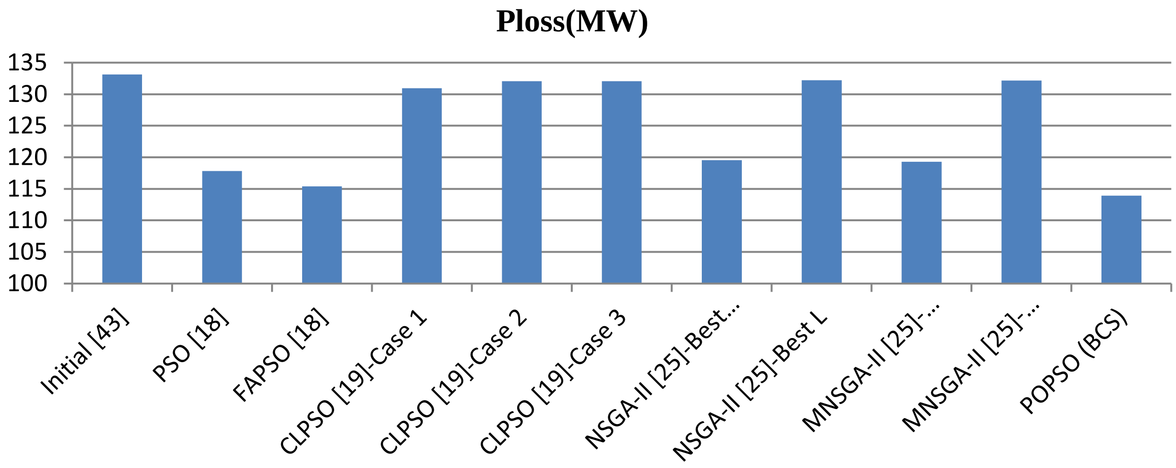

Figure 12. Comparison results of power loss in IEEE 118-bus test system

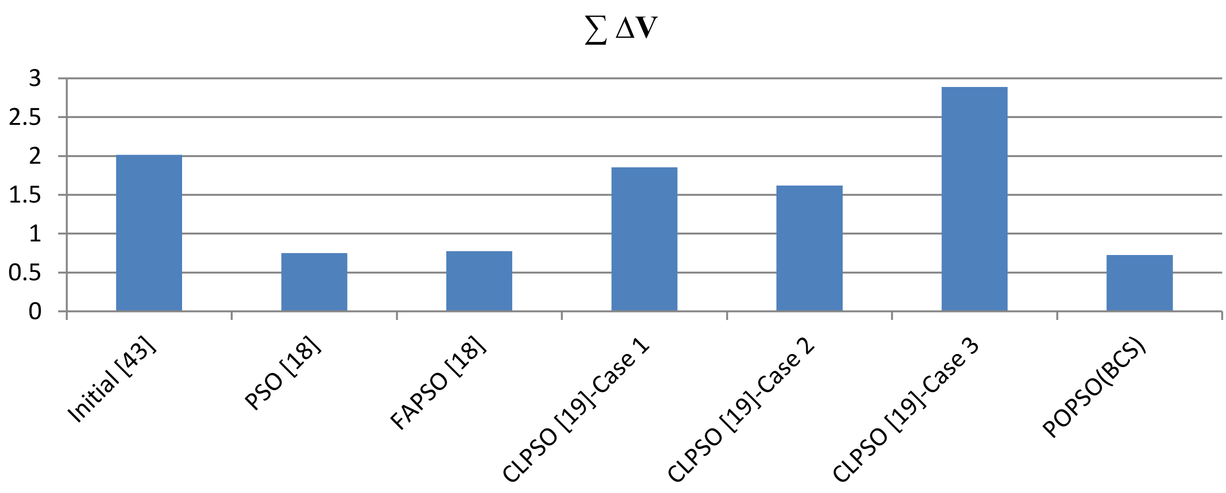

Figure 13. Comparison results of voltage deviation in IEEE 118-bus test system

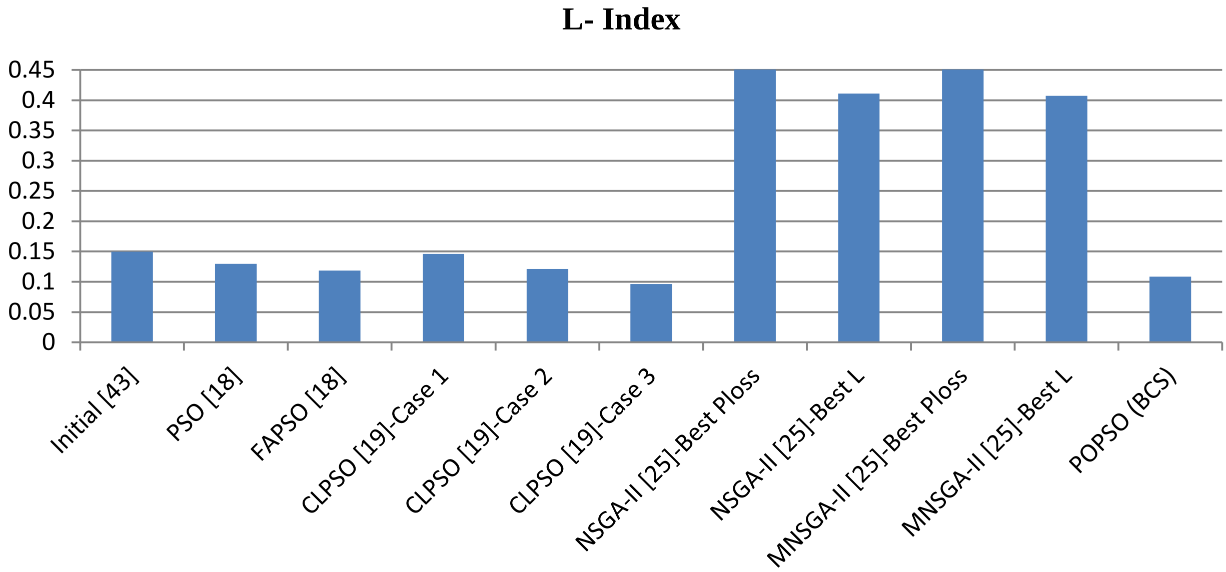

Figure 14. Comparison results of *L*-index in IEEE 118-bus test system

References

[1] Deeb, N., S. M. Shaidepour, "Linear reactive power optimization in a large power network using the decomposition approach", IEEE Trans. Power System, vol. 5, no. 2, pp. 428–35, 1990.

[2] Granville, S. "Optimal reactive dispatch through interior point methods", IEEE Trans. Power System, vol. 9, no. 1, pp. 136–46, 1994.

[3] Gomes, J. R, O. R. Saavedra, "A Cauchy-based evolution strategy for solving the reactive power dispatch problem", International Journal Electrical Power and Energy System, vol. 24, no. 4, pp. 277–83, 2002.

[4] Bhagwan, D. D., C. Patvardhan, "Reactive power dispatch with a hybrid stochastic search technique", International Journal Electrical Power and Energy System, vol. 24, no. 9, pp. 731–6, 2002.

[5] Devaraj, D., "Improved genetic algorithm for multi-objective reactive power dispatch problem", European Trans. on Electrical Power, vol. 17, no. 6, pp. 569-581, 2007.

[6] Liu, Y. T., L. Ma, J.J. Zhang, "Reactive power optimization by GA/SA/TS combined algorithms", International Journal Electrical Power and Energy System, vol. 24, no. 9, pp. 765–9, 2002.

[7] Tomsovic, K., "A fuzzy linear programming approach to the reactive power/ voltage control problem", IEEE Trans. Power System, vol. 7, no. 1, pp. 287–93, 1992.

[8] Grudinin, N. "Reactive power optimization using successive quadratic programming method", IEEE Trans Power System, vol. 13, no. 4, pp. 1219–25, 1998.

[9] Abido, M. A., J.M. Bakhashwain, "Optimal VAR dispatch using a multi-objective evolutionary algorithm", International Journal Electrical Power and Energy System, vol. 27, no. 1, pp. 13-20, 2005.

[10] Jiang, C., C. Wang, "Improved evolutionary programming with dynamic mutation and metropolis criteria for multi-objective reactive power optimization", IEE Proc Generation Transmission Distribution, vol. 152, no. 2, pp. 291–4, 2005.

[11] Zhou, A., B-Y. Qu, H. Li, S-Z. Zhao, P. N. Suganthan, Q. Zhang, "Multiobjective Evolutionary Algorithms: A Survey of the State-of-the-art", Swarm and Evolutionary Computation, vol. 1, no. 1, pp. 32-49, 2011.

[12] Aribia, H. B., N. Derbel, H.H. Abdallah, "The active–reactive – complete dispatch of an electrical network", International Journal of Electrical Power and Energy Systems, vol. 44, no. 1, pp. 236-248, 2013.

[13] Pires, D. F., C. H. Antunes, A. G. Martins, "NSGA-II with local search for a multi-objective reactive power compensation problem", International Journal of Electrical Power and Energy Systems, vol. 43, no. 1, pp. 313-324, 2012.

[14] Wu, Q. H. , Y.J. Cao, J.Y. Wen, "Optimal reactive power dispatch using an adaptive genetic algorithm", International Journal Electrical Power and Energy System, vol. 20, no. 8, pp. 563–569, 1998.

[15] del Valle, Y. et al., "Particle swarm optimization: basic concepts, variants and applications in power systems", IEEE Trans. Evol. Comput., vol. 12, no. 2, pp. 171–195, 2008.

[16] Esmin, A. A. A., G. Lambert-Torres, A. C. Zambroni de Souza, "A hybrid particle swarm optimization applied to loss power minimization", IEEE Trans. Power System, vol. 20, no. 2, pp. 859–869, 2005.

[17] Vlachogiannis, J. G., K. Y. Lee, "A comparative study on particle swarm optimization for optimal steady-state performance of power systems", IEEE Trans. Power System, vol. 21, no. 4, pp. 1718–1728, 2006.

[18] Zhang, W., Y. Liu, "Multi-objective reactive power and voltage control based on fuzzy optimization strategy and fuzzy adaptive particle swarm", International

Journal Electrical Power and Energy System, vol. 30, no. 9, pp. 525–532, 2008.

[19] Mahadevan, K., P. S. Kannan, "Comprehensive learning particle swarm optimization for reactive power dispatch", International Journal Applied Soft Computing, vol. 10, no. 2, pp. 641–652, 2010.

[20] Varadarajan, M., K. S. Swarup, "Network loss minimization with voltage security using differential evolution", Electric Power System Res., vol. 78, no. 5, pp. 815–823, 2008.

[21] Varadarajan, M., K. S. Swarup, "Differential evolutionary algorithm for optimal reactive power dispatch", International Journal Electrical Power and Energy System, vol. 30, no. 8, pp. 435–441, 2008.

[22] Abou El Ela, A. A., M. A. Abido, S.R. Spea, "Differential evolution algorithm for optimal reactive power dispatch", Electric Power System Research, vol. 81, no. 2, pp. 458-464, 2011.

[23] Dai, Ch., W. Chen, Y. Zhu, X. Zhang "Reactive power dispatch considering voltage stability with seeker optimization algorithm" International Journal of Electrical Power & Energy Systems, vol. 79, no. 10, pp. 1462-1471, 2009.

[24] Zhihuan, L., L. Yinhong, D. Xianzhong, "Non-dominated sorting genetic algorithm-II for robust multi-objective optimal reactive power dispatch", IET Generation, Transmission & Distribution, vol. 4, no. 9, pp. 1000 – 1008, 2010.

[25] Jeyadevi, S., S. Baskar, C. K. Babulal, M. Willjuice Iruthayarajan, "Solving multi-objective optimal reactive power dispatch using modified NSGA-II", International Journal of Electrical Power and Energy Systems, vol. 33, no. 2, pp. 219-228, 2011.

[26] Kennedy, J., R.C. Eberhart, "Particle swarm optimization", Proc IEEE Int. Conf. Neural Networks, vol. 4, pp. 1942–8, 1995.

[27] Yoshida, H., K. Kawata, Y. Fukuyama, S. Takayama, Y. Nakanishi, "A particle swarm optimization for reactive power and voltage control considering voltage security assessment", IEEE Trans. Power System, vol. 15, no. 4, pp. 1232–9, 2000.

[28] Abido, M. A., "Optimal power flow using particle swarm optimization", International Journal Electrical Power and Energy System, vol. 24, no. 7, pp. 563–71, 2002.

[29] Kassabalidis, I. N., M. A. El-Sharkawi, R. Marks, L.S. Moulin, A.P. Alves da Silva, "Dynamic security border identification using enhanced particle swarm optimization", IEEE Trans. Power System, vol. 17, no. 3, pp. 723–9, 2002.

[30] Naka, S., T. Genji, T. Yura, Y. Fukuyama, "A hybrid particle swarm optimization for distribution state estimation", IEEE Trans. Power System, vol. 18, no. 1, pp. 60–68, 2003.

[31] Ngatchou, P., A. Zarei, A. El-Sharkawi, "Pareto multi objective optimization", Intelligent Systems Application to Power Systems, Proceedings of the 13th International Conference on 6-10 Nov. 2005, pp. 84 – 91.

[32] Montoya, F. G., et al., "Minimization of voltage deviation and power losses in power networks using Pareto optimization methods", Engineering Applications of Artificial Intelligence, vol. 23, no. 5, pp. 695-703, 2010.

[33] Yassami, H., A. Darabi, S. M. R. Rafiei, "Power system stabilizer design using Strength Pareto multi-objective optimization approach", Electric Power Systems Research, vol. 80, no. 7, pp. 838–846, 2010.

[34] Balamourougan, V., T.S. Sidhu, M. S. Sachdev, "Technique for online prediction of voltage collapse", IEE Proc. Gen. Trans. Distrib., vol. 151, no. 4, pp. 453-460, 2004.

[35] Hugang, X., C. Haozhong, L. Haiyu, "Optimal reactive power flow incorporating static voltage stability based on multi-objective adaptive immune algorithm", Energy Conversion and Management, vol. 49, no. 5, pp. 1175–1181, 2008.

[36] Kessel, P., H.Glavitsch, "Estimating the voltage stability of a power system", IEEE Trans Power Del., vol. 1, no. 3, pp. 346–54, 1986.

[37] Tuan, T. Q., J. Fandino, N. Hadjsaid, J.C. Sabonnadiere, H. Vu, "Emergency load shedding to avoid risk of voltage instability using indicators", IEEE Trans Power System, vol. 9, no. 1, pp. 341–8, 1994.

[38] Kennedy, J., "The particle swarm: Social adaptation of knowledge," in Proc. IEEE Int. Conf. Evolutionary Comp., Indianapolis, IN, pp. 303–308, 1997.

[39] Shi, Y., R.C. Eberhart, "A modified particle swarm optimizer", In: Proceedings of the IEEE international Conference Evolutionary Computation, pp. 69–73, 1998.

[40] Carlisle, A., G. Dozier, "An off-the-shelf PSO", In: Proceedings of the IEEE International Workshop Particle Swarm Optimization, USA, pp. 1–6, 2001.

[41] Sharaf, A. M., A.A.A. El-Gammal, "A multi objective multi-stage particle swarm optimization MOPSO search scheme for power quality and loss reduction on radial distribution system", International Conference on Renewable Energies and Power Quality, 2009.

[42] Dhillon, J. S., S.C. Parti, D.P. Kothari, "Stochastic economic emission load dispatch", Electric Power System Research, vol. 26, no. 3, pp. 179–86, 1993.

[43] Power System Test Case Archive, December [Online], Available: http://www.ee.washington.edu/research/pstca/, 2006.